Does the Android Operating System Provide what the MEMS-IMU Manufacturers Promise?

M. Bochkati[1], T. Pany[1]

[1] Institute of Space Technology and Space Applications, Bundeswehr University Munich
Werner-Heisenberg-Weg 39
85577 Neubiberg
GERMANY

Inertial Sensors and Systems 2021
Braunschweig, Germany

978-1-6654-3178-1/21/$31.00 ©2021 IEEE

Abstract

Beside the camera, MEMS IMUs (Micro Elector-Mechanical Systems) belong today to the standard sensor conglomerate that every smartphone should have. In the future, the importance of MEMS-IMUs will increase more and more, especially if we talk about smart cities or internet of things (IoT). Since the MEMS manufacturer care only about numbers, i.e., low-cost, size and power consumption, some hardware and software integration deficits are highly likely to happen during the assemblage of the cell phone. This paper aims to check the quality of the consumer-grade smartphone IMUs from the user point of view. This includes the communication between the Android OS and the motion sensor. Additionally, a laboratory calibration of a couple of Xiaomi Mi 8 smartphones together with the same IMU-chip provided directly from the manufacturer has been performed. Referring to the spec. sheets, the outcome of the calibration (i.e., bias, scale factor and non-orthogonality errors) reveals, that the quality of both accelerometer and gyroscope parameters outperforms the manufacturer specifications. However, the only parameter that failed during this test is the bias error of the gyroscope. Further analysis of the stochastic processes show an unexpected behavior in the accelerometer z-axis for all employed smartphones, which can be caused by the electromagnetic compatibility or power supply regulation issues.

1. Introduction

In the last two decades, the market share of the MEMS IMUs (Micro Elector-Mechanical Systems) has been growing immensely, especially as the smartphone manufacturers have become aware of the unlimited potential of these miniaturized devices that did revolutionize our life. Thanks to their capabilities, various entertainment features, such as augmented reality (AR) using smartphones as well as their navigation applications, e.g., pedestrian navigation, are possible today. As low-cost single-frequency GNSS chips has been integrated into the mobile phones, the fusion with the MEMS-IMUs becomes more attractive due to their complementary behaviour. In 2008, the first Android operating system was published, which paved the way for a rapid development of the smartphone-based navigation applications dedicated for both indoor and outdoor areas. Since then, every user, with Android programming skills could interact with all available sensors in his smartphone to implement his own application (App). Uncountable scientific publications have already investigated the characteristics of the GNSS receiver integrated into a smartphone and its behaviour. Some decimetre accuracy can be achieved under optimal environmental conditions. In 2018, the world's first dual-frequency (L1/E1 & L5/E5) smartphone, Xiaomi Mi 8 [1], fitted with a Broadcom BCM47755 chip was introduced, which arouse an enormous

enthusiasm among the PNT community. Having dual-frequency GNSS-observation allows to cancels out the common errors such as multipath (MP) or atmospheric influences. Thanks to this option, some researchers were able to achieve 2 cm RTK-accuracy for a static scenario which is competitive with geodetic commercial receivers that cost thousands of dollars. However, this accuracy was possible only with special set-up that could either shield the smartphone antenna form the surrounding multipath, for example using a choke-ring [2], or a development kit form the GNSS-Chip manufacturer, Broadcom, that allows to connect the GNSS receiver to an external higher-grade antenna [3]. The advantage of the second example is to decuple the GNSS-chip from the smartphone environment to avoid possible interference from the electronic environment and therefore only the original behaviour of the chip can be investigated. Based on this approach, if also a development kit of the Smartphone MEMS-IMU is available, the Android system can be avoided and thus only the raw data of both accelerometer and gyroscope as the MEMS-chip manufacturer delivers, can be analysed, and compared with the smartphone observations.

This contribution aims to compare both stochastic and constant error parameters between smartphone IMU and the same/similar device hosted by a development kit that can be obtained directly from the MEMS-IMU manufacturer. Additionally, to provide a fair comparison, the calibration procedures took place in our inertial laboratory at the Universität der Bundeswehr München (UniBwM). The devices under test are, as stated before, 4 the dual-frequency Xiaomi Mi 8 that incorporates a MEMS-IMU from TDK-InvenSense, namely ICM-20690 [4] and on the other hand 4 development kits for ICM-20602 (DK-20602) [5]. The reason why the DK-20602 was selected, is that the ICM-20690 IMU-chip is available only for mass market applications and therefore no developer kit (DK) is offered for single users. Intensive investigation of the different spec sheets from the same manufacture revealed that the ICM- 20602 has the same specifications. These 8 units underwent different test, such as 6-Position Static Test to estimate the accelerometer bias, scale factor (SF) and non-orthogonality error and for the gyroscope only the bias and non-orthogonality calibration parameters. To estimate the gyroscope SF error angular Rate Tests (ART) with constant angle velocity of 60 deg/s have been conducted. Additionally, to investigate the stochastic behaviour of these sensors, short static data sets for approx. 15 minutes @100Hz have been collected and afterwards analysed by means of the Allan-Variance (AVAR) methodology.

The remainder of this paper is structured as follow. Section 2 describes the communication issue between IMU and Android OS. Afterwards the calibration setup in the inertial laboratory will be briefly described. Then, two IMU calibration techniques, namely the Six-Position-Static test and the Angle Rate test will be introduced. Subsequently, the achieved calibration results will be analysed and discussed. Finally, a brief assessment of the IMU stochastic behavior by means of the AVAR methodology will be done.

2. Communication Issue Between IMU and Android OS

To acquire the IMU sensor data as fast as possible, i.e,. with the lowest latency, the method ”SENSOR_DELAY_FASTEST” which represents a method of the Android class “*SensorManager*” was implemented in the our GNSS/IMU logger app [6] (Fig. 1).

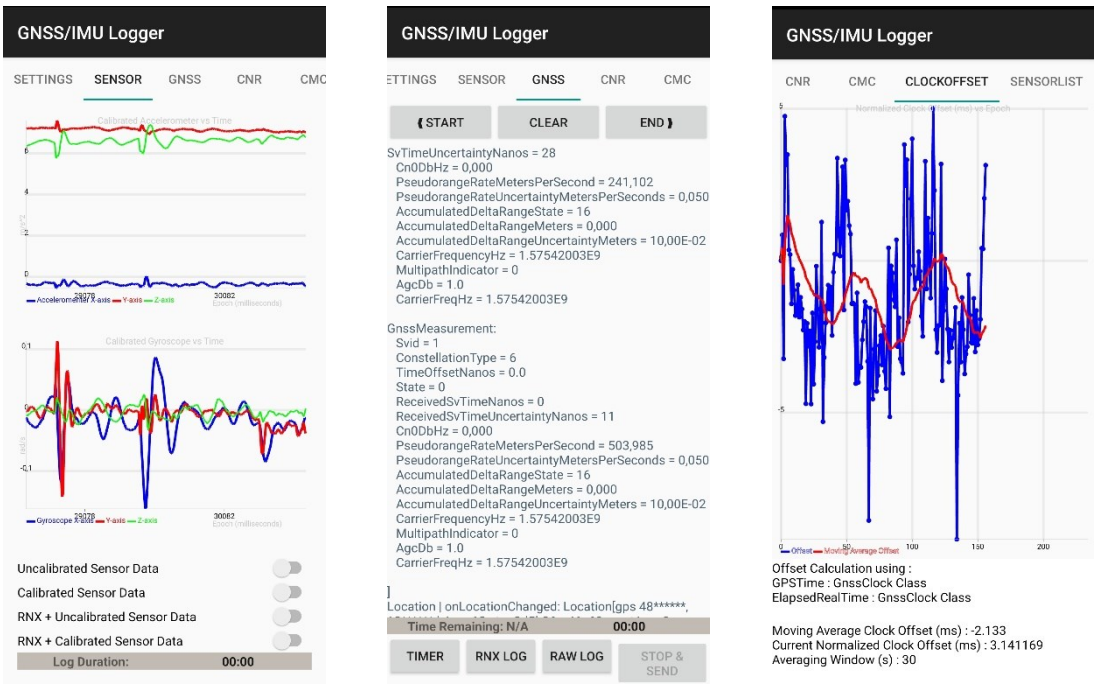

Figure 1: Screenshots of GNSS/IMU logger app (version: v2.1.0.1)

After collecting different static data using many Xiaomi Mi8 smartphones and considering the manufacturer output data rates of the incorporate ICM-20690 chip (see Tab. 1) the sampling rates of both accelerometer and gyroscope jump between two main frequencies, namely 500 Hz and 333.33 Hz (see Fig.2). Obviously, it exists a communication problem between the Android operating system (in our case Android 10) and the IMU chip, so that the incoming time of both sensors are somehow exchanged. Without having the knowledge about the smartphone IMU chip and therefore the corresponding manufacturer specifications, the user will make average of both sampling rates, which may have an impact

of the performance, especially when it comes to explorer the stochastic behavior the MEMS-device and try to estimate the noise parameters such random walk (RW) error amplitude.

Table 1: Manufacturer Specification of ICM-20690 MEMS IMU built in Xiaomi Mi8 Smartphones [4]

Parameter	Accelerometer	Gyroscope	Conditions
Bias error	±40 mg	±1 $\mathrm{deg/s}$	Board-level, all axes @ 25°C
Scale Factor	±1 %	±1 %	@ 25°C
Cross-Axis Sensitivity	±1 %	±1 %	
Full-Scale Range	±8 g	±1000 $\mathrm{deg/s}$	
Noise Density	100 $\mu g/\sqrt{\mathrm{Hz}}$	0.004 $\mathrm{deg/s}/\sqrt{\mathrm{Hz}}$	@ 10 Hz
Output Data Rate	500 Hz	333.33 Hz	Low Power Mode

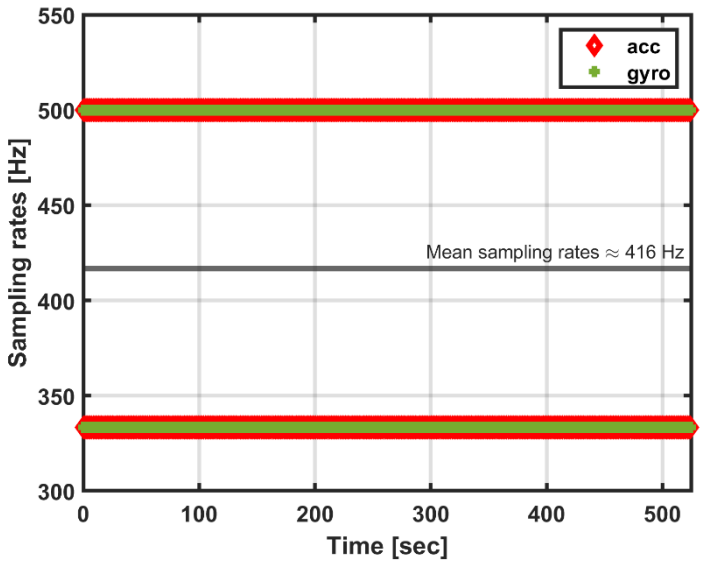

Figure 2: sampling rates derived directly from the time vector of both accelerometer and gyroscope collected by means of GNSS/IMU logger

Fig. 3 shows an example what happens when assumed another sampling rates as the IMU in reality provides. There two Allan-variance sequences are estimated for one Mi 8 accelerometer-axis. While the blue curve shows the AVAR estimated using the true sampling rates as indicated by the manufacturer, the red one is shifted slightly to the right when assuming a wrong frequency, which is in our case approx. 416 Hz (see Fig. 1).

Consequently, an error in the estimation of the white noise amplitude (determined as the intersection of -1/2 slope with the 1 s vertical line) will happen

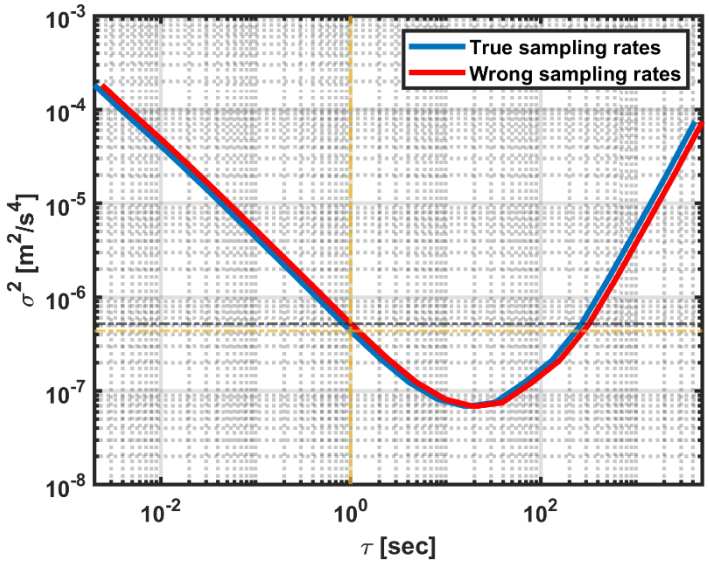

Figure 3: example of an accelerometer Allan-variance sequence computed with true (500 Hz) and with assumed wrong frequency (416 Hz)

In order to exclude a possible implementation bug in our Android logger during the IMU acquisition two other open-source Android applications [7] [8], that provides the same method, i.e. ”SENSOR_DELAY_FASTEST”, were employed to verify this suspicious behaviour. After collecting a bunch of IMU observations with different Mi 8 devices, the same timing/communication issue popped up.

3. Experimental Setup and IMU Calibration

In this section a comparison between the estimated deterministic calibration parameters obtained from the Mi 8 Smartphones and the TDK DK-ICM20602 as reference hardware is performed. This includes the constant bias, scale factor and non-orthogonality (N) errors. Additionally, an accuracy assessment of these results will be made based on the manufacture specifications. To guarantee a fair comparison between all under-test MEMS-IMU devices, a calibration under controlled laboratory conditions is therefore mandatory.

To this end, the standard high accurate Six-Position Static Test (SPST) as well as Angle Rate Test (ART) were performed by means of our 3-axis motion simulator from the company “*Acuitas AG*” [9], which provides all necessary reference signals such as rotation rates which the highest accuracy. Furthermore, for a high accurate calibration of the MEMS-accelerometer the reference gravity with an accuracy of 3-4 µGal ($\approx 3 \cdot 10^{-8} \frac{m}{s^2}$) is available.

In this experiment 4x Mi8 smartphones and 4x TDK DK-ICM20602 manufacturer development boards have been calibrated. During this process the laboratory temperature was kept as constant as possible @ 27°C (no climate chamber was used for temperature stabilization!). The ISTA GNSS/IMU logger and the TDK InvenSense MotionLink (release 4.1.8) [10], a GUI based sensor evaluation tool, were used to collect the raw uncalibrated IMU data of the ICM-20690 and DK-20602 respectively, as can be seen in Fig. 4

Figure 4: used tools to collect uncalibrated IMU data, TDK InvenSense MotionLink (left) and GNSS/IMU logger (right)

In the MotionLink interface (left subfigure) the same specification as read from senor list provided by the Android OS, such as accelerometer and gyroscope full scale range (FSR), were setup to generate similar conditions in both devices. In case of the Mi 8 the accelerometer FSR was equal to 8 g while for the gyro the FSR value is 1000 deg/s.

Additionally, the IMU data from the DK-20602 were collected @100 Hz during the calibration procedure. Figure 5 shows the mounting of these sensors as preparation for the calibration tasks.

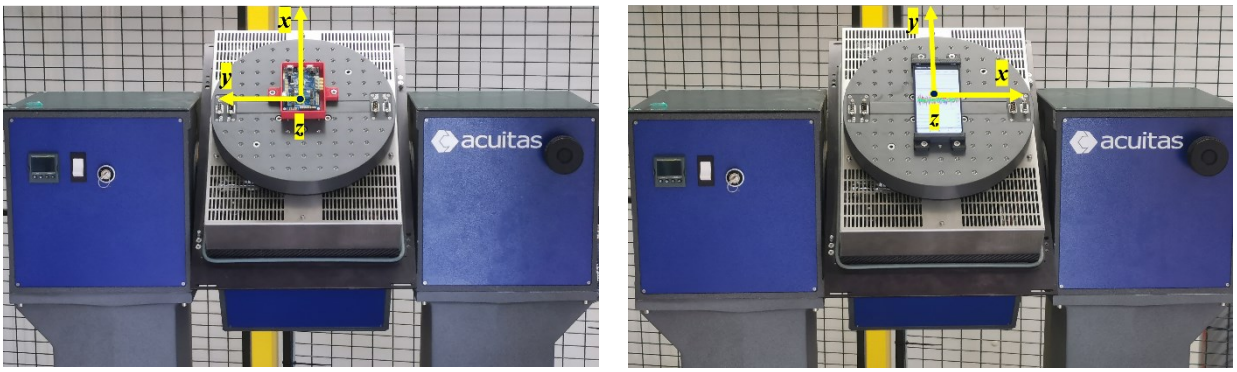

Figure 5: TDK DK-20602 (left) and Xiaomi Mi 8 (right) mounted on the three-axis turntable

3.1. Six-Position Static Test

According to [10], the Six-Position Static Test methodology consists of mounting the inertial system on a leveled surface with sensitive x-, y-, and z-axes of the IMU pointing alternately up and down which results in a total of 6 different positions. This enables to compute for each triad component both bias and scale factor errors that can be mathematically formulated by the following two equations:

$$b = \frac{l_f^{up} + l_f^{\text{down}}}{2} \tag{1}$$

$$S = \frac{l_f^{up} - l_f^{\text{down}} - 2 \cdot K}{2 \cdot K} \tag{2}$$

Where l_f^{up} and l_f^{down} represent the sensor measurement with the sensitive axis pointing upwards and downwards respectively. K is the known reference signal which can be either the local gravity constant or the magnitude of the Earth's rotation rate. However, the earth rotation rate can only be used for navigation and tactical grade gyroscopes since low grade gyroscopes such as MEMS suffer from bias instability and noise levels that can completely mask the earth's reference signal [12] [13]. As for low-cost IMU the non-orthogonality error become more considerable due to the manufacturing imperfection, the standard Six-Position Static Test is not able to estimate this parameter. In [14] an improved six-position test methodology was introduced which takes into account all three types of errors, i.e. bias, scale factor and non-orthogonality in a least squares (LSQ) adjustment process. In this approach the output of a triad of sensors (e.g., accelerometers) can be represented as

$$\begin{bmatrix} l_{ax} \\ l_{ay} \\ l_{az} \end{bmatrix} = \begin{bmatrix} S_{xx} & N_{xy} & N_{xz} \\ N_{yx} & S_{yy} & N_{yz} \\ N_{zx} & N_{zy} & S_{zz} \end{bmatrix} \begin{bmatrix} a_x \\ a_y \\ a_z \end{bmatrix} + \begin{bmatrix} b_{ax} \\ b_{ay} \\ b_{az} \end{bmatrix} \text{ or} \tag{3}$$

$$\begin{bmatrix} l_{ax} \\ l_{ay} \\ l_{az} \end{bmatrix} = \underbrace{\begin{bmatrix} S_{xx} & N_{xy} & N_{xz} & b_{ax} \\ N_{yx} & S_{yy} & N_{yz} & b_{ay} \\ N_{zx} & N_{zy} & S_{zz} & b_{az} \end{bmatrix}}_{\boldsymbol{M}} \underbrace{\begin{bmatrix} a_x \\ a_y \\ a_z \\ 1 \end{bmatrix}}_{a} \tag{4}$$

where the diagonal $\boldsymbol{S}$ elements represent the scale factors, the off-diagonal elements $\boldsymbol{N}$ are the nonorthogonalities between two different axes, and the $\boldsymbol{b}$ components are the biases. By aligning the IMU triad using the standard 6-position method to the reference normal gravity g , the ideal accelerations would be measured as:

$$a_1' = \begin{bmatrix} \mathrm{g} \\ 0 \\ 0 \end{bmatrix}, a_2' = \begin{bmatrix} -\mathrm{g} \\ 0 \\ 0 \end{bmatrix}, a_3' = \begin{bmatrix} 0 \\ \mathrm{g} \\ 0 \end{bmatrix}, a_4' = \begin{bmatrix} 0 \\ -\mathrm{g} \\ 0 \end{bmatrix}, a_5' = \begin{bmatrix} 0 \\ 0 \\ \mathrm{g} \end{bmatrix}, a_6' = \begin{bmatrix} 0 \\ 0 \\ -\mathrm{g} \end{bmatrix} \tag{5}$$

These observations can be then merged in the design matrix $\mathbf{A}$:

$$\mathbf{A} = \begin{pmatrix} a_1' & a_2' & a_3' & a_4' & a_5' & a_6' \\ 1 & 1 & 1 & 1 & 1 & 1 \end{pmatrix} \tag{6}$$

With the raw output of the accelerometer the matrix U can be built as

$$\mathbf{U} = [u_1 \quad u_2 \quad u_3 \quad u_4 \quad u_5 \quad u_6] \tag{7}$$

where
$$u_1 = \begin{bmatrix} l_{ax} \\ l_{ay} \\ l_{az} \end{bmatrix}_{Xaxis\_up}, u_2 = \begin{bmatrix} l_{ax} \\ l_{ay} \\ l_{az} \end{bmatrix}_{Xaxis\_down} \cdots \tag{8}$$

Finally, after applying a sum of multiplications of the introduced vectors and matrices, the matrix a $\mathbf{M}$ (see. Eq. 4) that contains the unknown calibration parameters can be generated as

$$\mathbf{M} = \mathbf{U} \cdot \mathbf{A}^{\boldsymbol{T}} \cdot (\mathbf{A}\mathbf{A}^{\boldsymbol{T}})^{-\mathbf{1}} \tag{9}$$

Figure 6 shows, exemplary, the IMU signal of one Mi 8 smartphone during the six-position static test, where in the left subplot the signal of the accelerometer, i.e., specific force $\boldsymbol{f}_{\mathrm{ib}}^{b}$ indicates the up (by around 10 m/s²) and down position (by around -9.81 m/s²). In the right subplot the signal of the gyroscope triad is depicted, where during the changes between up

and down position only the angle changes between 180 and -180 degrees (e.g., red peak at around 600 seconds.

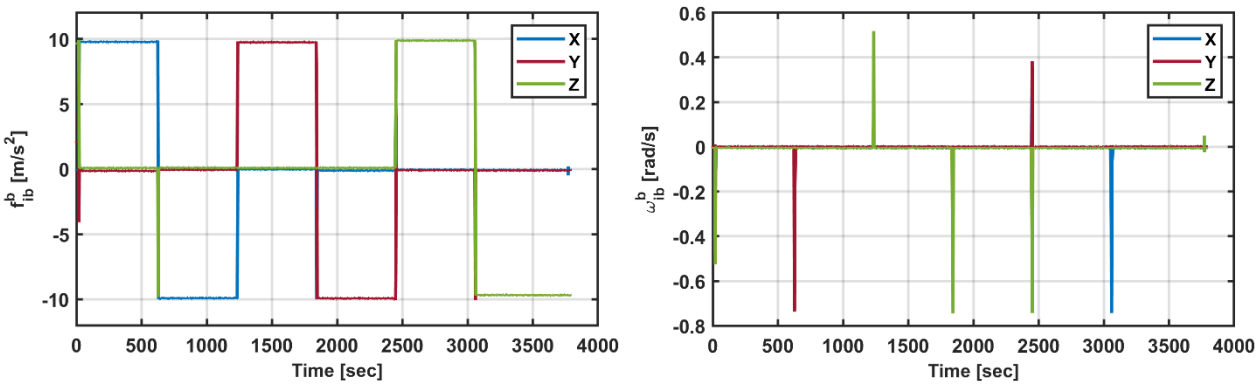

Figure 6: example of smartphone IMU output in six-position static test

For the gyroscope the only constant error parameter that can be estimated during this procedure is the bias value, which can be computed be means of equation 1.

3.2. Angle Rate Test

To estimate both scale factor and non-orthogonality errors of the gyroscope the ART can be applied, where the reference signal K is represented by a high accurate artificial rotation generated by the rotation table. Here, the IMU triad is mounted horizontally and rotated subsequently around each axis (usually pointing upwards) in clockwise (cw) and counterclockwise (ccw) sense (see Fig. 7). The output during these two opposite rotations is indicated in Eq. 10 as l_{i_cw} and l_{i_ccw}, where $i = x, y, z$. Comparing the gyroscope output with the reference signal the scale factor error S_{gi} can be computed

$$S_{gi} = \frac{l_{i\_cw} - l_{i\_ccw} - 2 \cdot K}{2 \cdot K} \tag{10}$$

$$N_{g,ij} = \frac{l_{ij\_cw} - l_{ij\_ccw}}{2 \cdot K} \tag{11}$$

The gyro non-orthogonality error, $N_{g,ij}$, are computed from the readings of the two axes (l_{ij_cw} and l_{ij_ccw}), that are levelled during the constant rotation around the upward pointing (third) axis. Assume, the rotation is around the x-axis, therefore the non-orthogonality between the x- and y-axis ($N_{g,xy}$) and non-orthogonality between the x- and the z-axis ($N_{g,xz}$) can be estimated.

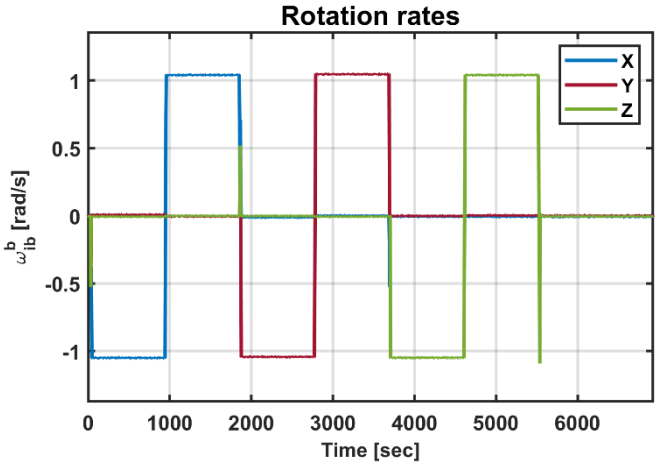

Figure 7: example of Smartphone IMU output during the gyro rate test @60 deg/s reference rotation

3.3. Results and Analysis

Table 2-5 list all calibration results achieved under laboratory conditions. When looking at the mean constant error of the accelerometer for both Mi 8 devices (Dev1 … Dev4) and the DK-20602 (DK1 … DK4) in Tab. 2 and 3 respectively, it appears that both units have the same quality, except some outlier in the non-orthogonally errors for the DK2 and DK4 (>1%). However, when comparing the mean value from both tables with the those of manufacturer specifications, as in Tab. 1, it becomes clear that the calibration outcome outperforms the reference specifications.

Table 2: Accelerometer calibration parameter estimated for 4x Xiaomi Mi8 smartphones

Mi 8	**Bias [mg]**			**Scale Factor [%]**			**Non-Orthogonality [%]**					
	b_{ax}	b_{ay}	b_{az}	S_{xx}	S_{yy}	S_{zz}	N_{xy}	N_{xz}	N_{yx}	N_{yz}	N_{zx}	N_{zy}
Dev1	-7.3	-11.8	8.6	0.1	0.3	-0.2	-0.4	0.1	0.4	0.3	0.1	-0.3
Dev2	-7.4	-13.1	5.8	0.2	0.2	-0.3	-0.1	-0.1	0.1	0.3	0.1	-0.2
Dev3	-6.9	-9.6	9.6	0.3	0.2	-0.3	0.4	0.1	-0.4	0.1	-0.1	-0.1
Dev4	-7.9	6.6	-2.5	0.1	0.3	-0.2	-0.2	0.1	0.2	-0.1	-0.1	0.1
Mean	-7.4	-7.0	5.4	0.2	0.3	-0.3	-0.1	0.1	0.1	0.2	0	-0.1

Table 3: Accelerometer calibration parameter estimated for 4x TDK DK-20602 reference platforms

DK	Bias [mg]			Scale Factor [%]			Non-Orthogonality [%]					
	b_{ax}	b_{ax}	b_{ax}	S_{xx}	S_{yy}	S_{zz}	N_{xy}	N_{xz}	N_{yx}	N_{yz}	N_{zx}	N_{zy}
DK1	-11.6	-5.76	22.6	0.1	0.3	0.2	-0.3	0.6	0.3	0.7	-0.5	-0.7
DK2	-5.6	-6.1	-13.0	0.2	0.3	0.2	-0.1	-0.2	0.1	1.4	0.4	-1.3
DK3	-6.2	-7.4	-19.4	0.2	0.2	0.4	1.0	0.1	-1.1	0.7	0.1	-0.9
DK4	-6.4	-13.1	-7.2	0.1	0.2	0.3	0.1	0.4	-0.1	1.6	-0.3	-1.6
Mean	-7.5	-8.1	-4.2	0.2	0.3	0.3	0.2	0.2	-0.2	1.1	-0.1	-1.1

Similarly, the gyroscope constant errors show similar quality. The comparison with the manufacturer specifications revels that, like the accelerometer triad, the SF and non-orthogonality are one order of magnitude better. In contradiction, the bias errors for all tested devices did not reach the expected value which is ±1 deg/s

Table 4: Gyroscope calibration parameter estimated for 4x Xiaomi Mi8 smartphones

Mi 8	Bias [deg/s]			Scale Factor [%]			Non-Orthogonality [%]					
	b_{gx}	b_{gx}	b_{gx}	S_{xx}	S_{yy}	S_{zz}	N_{xy}	N_{xz}	N_{yx}	N_{yz}	N_{zx}	N_{zy}
Dev1	-4.1	-6.7	4.8	-0.1	-0.4	-0.2	-0.3	-0.3	0.4	0.3	-0.2	-0.3
Dev2	-4.1	-7.4	3.3	-0.2	-0.3	-0.3	0.1	-0.1	0.2	0.3	0.3	-0.3
Dev3	-4.0	-5.4	5.4	-0.2	-0.3	-0.2	0.6	-0.3	-0.6	0.2	0.1	-0.2
Dev4	-4.5	3.6	-1.4	-0.1	-0.1	-0.3	-0.1	-0.2	0.2	0.1	0.2	-0.1
Mean	-4.2	-4.0	3.0	-0.2	-0.3	-0.3	0.1	-0.2	0.1	0.2	0.1	-0.2

Table 5: Gyroscope calibration parameter estimated for 4x TDK DK-20602 reference platforms

DK	Bias [deg/s]			Scale Factor [%]			Non-Orthogonality [%]					
	b_{gx}	b_{gx}	b_{gx}	S_{xx}	S_{yy}	S_{zz}	N_{xy}	N_{xz}	N_{yx}	N_{yz}	N_{zx}	N_{zy}
DK1	-6.5	-3.2	12.5	-0.4	-0.3	-0.4	-0.3	0.6	0.4	0.8	-0.6	-0.7
DK2	-3.2	-3.4	-7.4	-0.5	-0.3	-0.1	-0.2	-0.5	0.2	0.9	-0.1	-1.0
DK3	-3.6	-4.2	-10.9	-0.2	-0.1	-0.6	0.8	-0.2	-0.8	1.1	-0.2	-0.9
DK4	-3.7	-7.4	-4.1	-0.4	-0.4	-0.4	-0.1	0.2	-0.2	1.7	-0.5	-1.6
Mean	-4.2	-4.5	-2.5	-0.4	-0.3	-0.4	0.1	0.1	-0.1	1.1	-0.1	-1.0

4. Assessment of the IMU Stochastic Behavior

In previous publication [2] the stochastic modelling of two Mi 8 mobile phones has been shown against a commercial MEMS-IMU from the company “Xsens”, where the quality of the ICM-20690 IMU was surprisingly competitive with its opponent device. Furthermore, some noise coefficient, such VRW/ARW and Bias Instability (BI) have been deduced. But the most interesting observation, was the noise behaviour of the accelerometer z-axis which was completely different from other both axes. The possible explanation made in [2] is that such random behaviour of the Xiaomi Mi 8 z-axis can be found in the manufacturing process related to the MEMS technology. A three-axis MEMS accelerometer chip is able to sense accelerations as a reaction of the force applied to the chip housing. The change in movement is equivalent to the change of capacitance between the moving structure of the chip. To guarantee the sensitivity in all three directions, i.e. x, y and z, two proof masses are available, namely a XY-axis proof mass and Z-axis proof mass that detect the in-plane and out-of-plane accelerations respectively. Since we have access to the same MEMS-IMU chip, it is worthy to investigate again this behaviour and maybe validate or reject the assumption made there.

For this reason, we collected for almost 15 minutes at the same sampling rates mentioned before using all tested hardware in the previous sections, i.e., the DK-ICM20602 and the Mi8 with the ICM-20690 MEMS chip, static IMU signals. Afterwards, from these static data sets a short Allan-variance sequence has been estimated for both accelerometer and gyroscopes triad as depicted in Fig. 8 and 9. When looking at the stochastic processes of the accelerometer axes in the left plot in Fig.8 and 9, it is clear that the noise process buried

in the signal of the z-axes for all tested smartphones are different than x- and y-axes, which show the usual slopes, i.e., transition from white noise (slope -1/2) to BI (slope 0). The z-axes exhibit a kind of sinusoidal noise as defined in [15]. This behaviour becomes more suspicious and seems not to be caused by the IMU-Chip itself, if we look on the z-axes of the DKs, which show the same structure as the remaining axes. Hence this could be an integration issue during the smartphone manufacturing process or maybe a noise introduced by other electronic units.

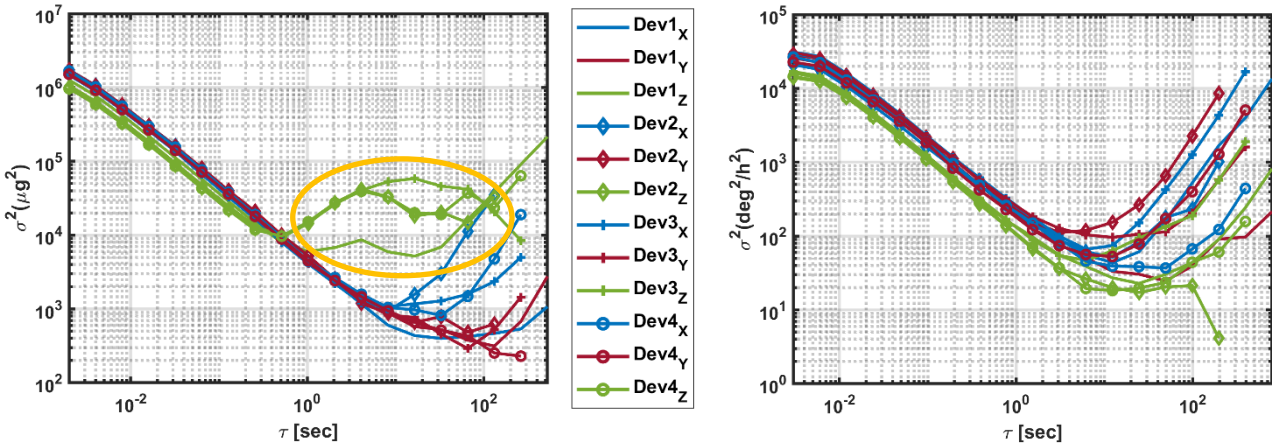

Figure 8: Allan-variance sequence estimated for 4 Xiaomi Mi8 IMUs @100 Hz, accelerometer (left) and gyroscope (right)

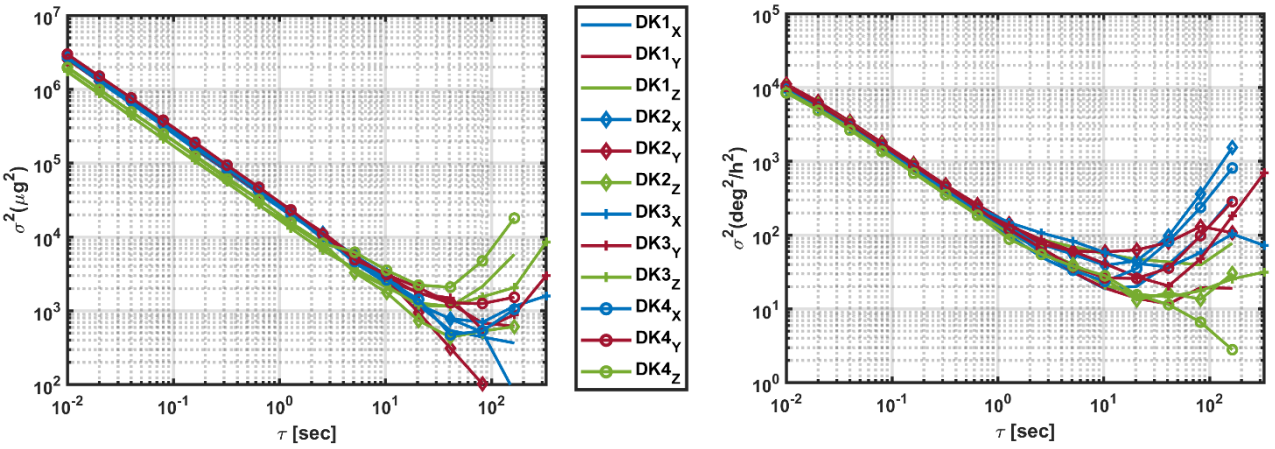

Figure 9: Allan-variance sequence estimated for 4x TDK DK-20602 development Kits @100 Hz, accelerometer (left) and gyroscope (right)

Despite this unexplained stochastic fluctuation in the smartphone's accelerometer axes, the rest of the AVAR-sequences shows the same random characteristics, in other words, all gyro axes in both platforms exhibit the same course, which includes WN (ARW/VRW) and

BI. However, the gyro axes of the reference hardware are overlapping each other perfectly, while the Mi 8 z-axes are less noisy.

5. Conclusion and Future Work

In this contribution, the integration quality of consumer grade inertial sensors in mass products, i.e. smartphones has been investigated. The first weak point that has been shown here, is the communication issue between the Android operating system the MEMS-IMU chip (ICM-20690) where it seems to be confused between the gyro and accelerometer time events. Additionally, comparison between cellphone-embedded IMU and the same type directly from the manufacturer under laboratory conditions reveals that the accelerometer constant errors, such as bias, scale factor and non-orthogonality are on the same level. However, these parameters were considerably smaller w.r.t. the manufacturer specification of the MEMS-Chip, which is in turn an advantage. Similarly, the comparison of the gyroscope deterministic errors shows the same quality as the reference developer board. The estimated smartphone gyro biases did not meet the ±1 deg/s from specifications. But, surprisingly, the SF and non-orthogonality error of this sensor was one order of magnitude smaller than expected. In term of stochastic processes, the most notably behaviour is that of the vertical accelerometer axis (z-axis) of the Mi 8 smartphone which is completely different from the reference developer kit.

Future works will include the update of the employed IMU logger to higher Android version, i.e., version 11 or higher which could solve the time event issue. Testing with other smartphones could also clarify the exact source of this problem. Furthermore, the quality of the computed calibration parameters can be assessed through a of GNSS/INS fusion. From the manufacturer side, processors with higher speed and better quality can handle the information flow of many sensors/ electronic unites without loss of information. We also assume, that better electromagnetic shielding of all built-in sensors could improve tolerance within the common smartphone casing significantly.

References

[1] Xiaomi Tech., “Mi 8 Specifications,” 2020. [Online]. Available*: https://www.mi.com/global/mi8/specs*. [Accessed 13 April 2020].

[2] M. Bochkati, H. Sharma, C. A. Lichtenberger and T. Pany, "Demonstration of Fused RTK (Fixed) + Inertial Positioning Using Android Smartphone Sensors Only," 2020 IEEE/ION Position, Location and Navigation Symposium (PLANS), 2020, pp. 1140-1154, doi: 10.1109/PLANS46316.2020.9109865.

[3] R. Riley, H. Landau, V. Gomez, N. Mishukova, W. Lentz and A. Clare, "Positioning with Android: GNSS observables", 2017 [Online]. Available*: https://www.gpsworld.com/positioning-with-android-gnss-observables/*. [Accessed 28 September 2021].

[4] InvenSense Inc., "ICM-20690 Datasheet," 2018. [Online]. Available: *https://invensense.tdk.com/wp-content/uploads/2016/10/DS-000178-ICM-20690-v1.0.pdf*. [Accessed 10 September 2021].

[5] InvenSense Inc., "DK-20602 SmartMotion Platform," 2018. [Online]. Available: *https://3cfeqx1hf82y3xcoull08ihx-wpengine.netdna-ssl.com/wpcontent/uploads/2017/11/SmartMotion_IntroTraining_customer_ver3.1.pdf*. [Accessed 26 August 2021].

[6] ISTA-UniBw M, "GNSS/IMU Logger (Version v2.1.0.1) [Android app]," 2021. [Online]. Available: *https://play.google.com/store/apps/details?id=com.ista.android.apps.location.gps.gnsslogger&hl=de&gl=US*. [Accessed 26 August 2021].

[7] Axel Lorenz, "Sensorstream IMU+GPS (Version 1.0) [Android app]," 2013. [Online]. Available: *https://play.google.com/store/apps/details?id=de.lorenz_fenster.sensorstreamgps&hl=de&gl=US*. [Accessed 22 August 2021].

[8] INNOVENTIONS, Inc., "Sensor Kinetics (Version 3.1.1) [Android app]," 2017. [Online]. Available: *https://play.google.com/store/apps/details?id=com.inventions.sensorkinetics&hl=de&gl=US*. [Accessed 22 August 2021].

[9] Acuitas AG, "Three Axis Motion Simulator Series "TEST FIXTURE SERIES TES-UUT-V_433-3-TG"," [Online]. Available: *https://www.acuitas.ch/application/files/8816/3058/2441/DS0013_1B_Three_Axis_Motion_Simulator_Series.pdf*. [Accessed 12 July 2021].

[10] InvenSense Inc., "SmartMotion Plattform - MotionLink," March 2018. [Online]. Available: *https://invensense.tdk.com/wpcontent/uploads/2017/11/SmartMotion_IntroTraining_customer_ver3.pdf*. [Accessed 10 September 2021].

[11] D. H. Titterton, and J. L. Weston, "Strapdown Inertial Navigation Technology", Second Edition, Stevenage, United Kingdom: IEE, 2004.

[12] P. Aggarwal, Z. Syed, X. Niu and N. El-Sheimy, “A Standard Testing and Calibration Procedure for Low Cost MEMS Inertial Sensors and Units,” Journal of Navigation, vol. 61, p. 323–336, March 2008.

[13] P. Aggarwal, Z. Syed, A. Noureldin and N. El-Sheimy, “MEMS-Based Integrated Navigation” (GNSS Technology and Applications), Artech House Publishers, 2010.

[14] E.-H. Shin and N. El-Sheimy, “A New Calibration Method For Strapdown Inertial Navigation Systems,” Zeitschrift für Geodäsie, Geoinformation und Landmanagement, vol. 127, p. 41–50, 2002.

[15] *IEEE Standard Specification Format Guide and Test Procedure for Single-Axis Interferometric Fiber Optic Gyros*, IEEE Std 952-1997, 1998, pp. 1-84.